



Machine Learning Models for Evaluation and Optimizing Evapotranspiration Prediction

Modelos de aprendizaje automático para evaluar y optimizar la predicción de la evapotranspiración

Deepak Kumar Raj ¹, and Gopikrishnan T ²

ABSTRACT

This study extensively analyzed three models, *i.e.*, M5P (model tree), ANFIS (adaptive neuro-fuzzy inference system), and GEP (gene expression programming), to predict actual evapotranspiration (ETo) at six major stations in the Mahanadi Basin region: Raipur, Korba, Jharsuguda, Bilaspur, Bhubaneswar, and Balangir. Evaluation metrics including the R^2 , RMSE, NSE, and MAE were applied to the testing dataset, revealing ANFIS's consistent superiority, with high R^2 (0.930746-0.990526) and NSE (0.926792-0.990458) values alongside the lowest RMSE (0.101152-0.332819) and MAE (0.000386-0.034319). Weighted scores confirmed ANFIS's dominance across multiple stations, except for specific instances: GEP excelled in Bhubaneswar and M5P in Balangir. This study highlighted ANFIS's proficiency in predicting ETo values across various locations, as demonstrated through the effective capture of variations in scatterplots. This underscores the importance of model selection, the versatility of machine learning models, and the effectiveness of combining artificial intelligence techniques for accurate ETo prediction. ANFIS consistently outperformed M5P and GEP, solidifying its status as a reliable prediction tool. While acknowledging the potential of M5P and GEP in specific contexts, this study stresses the need to tailor models to unique location characteristics. References to related studies supported the effectiveness of hybridized AI approaches in improving ETo modeling. We encourage ongoing research to refine the models, incorporate additional factors, and enhance predictive accuracy. Our findings provide valuable insights for water resource management, irrigation planning, and agricultural decision-making across diverse locations.

Keywords: evapotranspiration, machine learning, ANFIS, GEP, M5P tree

RESUMEN

Este estudio analizó de manera exhaustiva tres modelos, *i.e.*, el árbol de modelo (M5P), el sistema de inferencia neuro-difuso adaptativo (ANFIS) y la programación de expresión génica (GEP), para predecir la evapotranspiración real (ETo) en seis estaciones principales de la cuenca del Mahanadi: Raipur, Korba, Jharsuguda, Bilaspur, Bhubaneswar y Balangir. Se aplicaron métricas de evaluación al conjunto de prueba, incluyendo el R^2 , el RMSE, la NSE y el MAE, lo que reveló la consistente superioridad de ANFIS, con valores altos de R^2 (0.930746-0.990526) y NSE (0.926792-0.990458), junto con los valores más bajos de RMSE (0.101152-0.332819) y MAE (0.000386-0.034319). Los puntajes ponderados obtenidos confirmaron el dominio de ANFIS en múltiples estaciones, salvo en casos específicos: GEP se destacó en Bhubaneswar y M5P en Balangir. Este estudio resaltó la capacidad de ANFIS para predecir valores de ETo en diversas ubicaciones, lo cual se evidenció en la captura efectiva de variaciones en los diagramas de dispersión. Esto subraya la importancia de la selección de modelos, la versatilidad de los modelos de aprendizaje automático y la eficacia de combinar técnicas de inteligencia artificial (IA) para una predicción precisa de la ETo. ANFIS superó de manera consistente a M5P y GEP, consolidando su condición de herramienta confiable de predicción. Si bien se reconoce el potencial de M5P y GEP en contextos específicos, este estudio enfatiza la necesidad de adaptar los modelos a las características propias de cada lugar. Referencias a estudios relacionados respaldaron la eficacia de los enfoques híbridos de IA para mejorar el modelado de la ETo. Se invita a la investigación continua para refinar los modelos, incorporar factores adicionales y mejorar la precisión predictiva. Nuestros hallazgos ofrecen perspectivas valiosas para la gestión de los recursos hídricos, la planificación del riego y la toma de decisiones agrícolas en diversas ubicaciones.

Palabras clave: evapotranspiración, aprendizaje automático, ANFIS, GEP, árbol M5P

Received: March 19th, 2024

Accepted: July 9th, 2025

Introduction

In the field of agriculture, the separation of water from the surface of moist soil is known as *evaporation*, while a similar process occurring through the pores of leaves is referred to as *transpiration*. Due to the challenges associated with distinguishing these two phenomena on farms, they are commonly treated as a combined variable known as

¹ Dr., National Institute of Technology Patna, Bihar, India. M.Tech., IIT (BHU) Varanasi, Uttar Pradesh, India. Affiliation: Department of Civil Engineering, National Institute of Technology Patna, Patna, Bihar, India. E-mail: dkraj.iitbhu2018@gmail.com

² Dr., Anna University Chennai, Tamil Nadu, India. M.E. - Geoinformatics, Anna University Chennai, Tamil Nadu, India. Affiliation: Department of Civil Engineering, National Institute of Technology Patna, Patna, Bihar, India. E-mail: gk-tphd@gmail.com



evapotranspiration. This integrated term encompasses not only the water vaporized from the agricultural land's surface, but also the water received through rain, irrigation, or dew drops on leaves. As evapotranspiration represents the water needs of plants, its accurate measurement and prediction hold great importance in agricultural and irrigation projects. By understanding and quantifying evapotranspiration, farmers and irrigation planners can effectively manage water resources to meet crop demands and ensure optimal growth and productivity [1].

In irrigated agriculture, water resource management relies heavily on the ability to accurately predict and understand various aspects of the hydrological cycle. One crucial component in this regard is the precise quantification of evapotranspiration (ETo). By gaining a thorough understanding of ETo, it becomes possible to design and manage efficient irrigation systems, simulate crop yields, assess the water balance, and effectively plan and allocate water resources. The accurate prediction of ETo plays a fundamental role in ensuring the sustainable and optimal utilization of water in agricultural practices [2].

ETo plays a very important role in the hydrological cycle, particularly in agricultural practices. Accurately estimating and predicting it is essential for effective water resource management, for irrigation planning, and for determining the water requirements of plants and crops. Future ETo forecasting and prediction provide useful information for creating, organizing, and putting water resource management plans into action. Monthly scale predictions offer a longer-term perspective on ETo changes, which is particularly beneficial for crops with growth periods spanning several months. Additionally, the monthly evapotranspiration rate is directly used in assessing agricultural droughts, using well-known indicators like the standardized precipitation-evapotranspiration index (SPEI) and the Palmer drought severity index (PDSI).

In recent years, data-driven models, including stochastic and artificial intelligence (AI) methods, have demonstrated their efficacy in modeling and predicting hydrometeorological variables, offering efficient approaches for ETo modeling and forecasting. These models have shown promising performance and offer valuable tools for studying and predicting ETo variations at different spatiotemporal scales [3], [4], [5]. Accurate ETo prediction holds immense significance, particularly in regions that face limited water resources (e.g., Iran). It plays a pivotal role in determining suitable cultivation patterns and ensuring an efficient management of water and soil resources.

In Iran, two types of numerical models (stochastic and AI) have been employed to forecast ETo. [6] conducted a study in the humid areas of the Caspian Sea's southern margin, specifically the Guilan province, utilizing SARIMA (seasonal autoregressive integrated moving average), GMDH (group method of data handling), and SVM (support vector machine) models for ETo prediction. This research

showcased the application of diverse modeling techniques to estimate ETo accurately in a region characterized by high humidity. By employing these models, the researchers could acquire valuable insights into water management strategies, enabling the optimization of resources under the unique environmental conditions and agricultural practices of the region.

Within the domain of ETo modeling, numerous studies have delved into the effectiveness of both simple and hybridized AI approaches, highlighting the significant contributions made by researchers such as [6], [7], [8], [9], and [10]. These studies have provided compelling evidence that supports the integration of AI techniques for precise ETo prediction, aligning with the findings of this study. By using various AI methodologies, including machine learning algorithms and neural networks, these researchers have shown the immense potential of AI-driven approaches in advancing ETo modeling, allowing for a deeper understanding of its complex dynamics. These investigations have paved the way for further advancements in prediction and have expanded our knowledge and use of AI techniques in improving water resource management and agricultural planning.

The purpose of this paper is to evaluate and compare the performance of three different models, namely M5P, ANFIS, and GEP, for predicting actual ETo values by means of a provided dataset. The objective is to assess the accuracy and reliability of these models in estimating ETo, which is a crucial parameter in agricultural and water resource management. By analyzing multiple evaluation metrics such as R^2 , RMSE, NSE, and MAE, we seek to determine the most effective prediction model. The findings of this research can contribute to the selection and implementation of suitable models for ETo estimation, allowing for better decision-making processes regarding irrigation scheduling, crop yield forecasting, and water allocation in agricultural and environmental planning.

Materials and methods

Study area and data collection

The Mahanadi River holds significant importance as one of India's major river basins. Spanning a vast catchment area of 1.41 lakh km² ($\approx 141\,000$ km²), it flows through five states within the country. The river plays a crucial role in meeting various sectoral demands, such as irrigation, industry, recreation, and domestic usage. Mahanadi River Basin irrigation plays a vital role in agriculture and food production by providing a consistent water supply, extending the arable land, supporting crop diversification, mitigating drought impacts, and ensuring a stable food production. With controlled water application, it enhances crop yield and quality, reduces crop risks, and enables year-round cultivation. With a total length of approximately 858 km, the Mahanadi River hosts numerous multipurpose water resource projects, which are primarily aimed at

irrigating paddy crops in Chhattisgarh and Odisha. Among its noteworthy tributaries are the Hasdeo, Seonath, Mand, Ib, Ong, Tel, and Jonk Rivers. To harness the potential of the Mahanadi River, several water resource works have been constructed, including the Ravishankar Sagar, Tandula, Parry, Jonk, Hasdeo Bango, Kharang, Kodar, Mand, Maniyari, Hirakud, and Hasdeo Bango projects. These initiatives seek to optimize the utilization of the river's water resources and contribute to the overall development of the region [11]. The Mahanadi Basin is geographically located between 80°30' to 86°50' E longitudes and 19°20' to 23°35' N latitudes. This region experiences a subtropical climate with distinct seasonal variations. During the winter months of December to January, the minimum temperatures can decrease to approximately 4 °C, while, in May, the temperatures reach around 45°C, marking the peak of the summer. The basin receives an annual average rainfall of approximately 1200 mm, primarily during the monsoon season spanning from June to October. However, it is worth noting that the distribution of rainfall across the Mahanadi Basin is uneven due to factors such as vegetation and land use (including deforestation), which impact rainfall patterns. Additionally, global climate change, driven by greenhouse gas emissions, can lead to widespread alterations in precipitation and extreme weather events, resulting in varying precipitation levels in different areas [12]. This study was carried out in the Raipur, Korba, Jharsuguda, Bilaspur, Bhubaneswar, and Balangir district areas (Fig. 1).

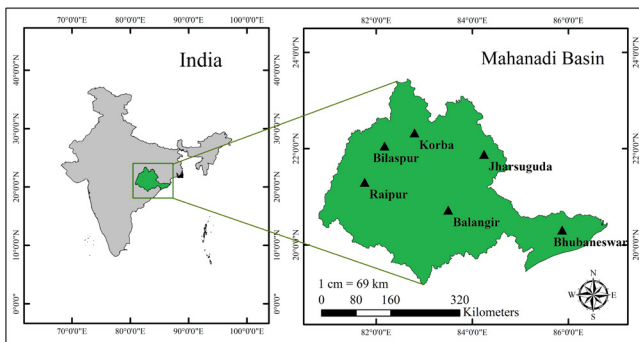


Figure 1. Location of the stations in the Mahanadi Basin
Source: Authors

We utilized a dataset containing monthly meteorological data from 1996 to 2020. This dataset includes various variables such as the minimum air temperature (T_{min}), the maximum air temperature (T_{max}), precipitation, the groundwater table, wind speed, downward shortwave radiation, vapor pressure, soil moisture, and actual ET_o . During the initial analysis, we identified a few missing values in the groundwater table data. To address this problem, we applied an averaging method to fill in the missing values and remove any errors. This refinement process improved the quality of our dataset by removing errors and incomplete data. This made our data more reliable and accurate for our research findings.

We used Google Earth Engine (GEE) data to extract monthly data for the aforementioned variables from

TerraClimate. This website provides reliable climate data on a global scale with a spatial resolution of approximately 4 km (0.04 degrees). TerraClimate is a high-resolution climate dataset that captures long-term climate patterns and variability. It is suitable for climate monitoring, research, and modeling. With it, researchers can analyze and understand climatic conditions at both regional and global levels [13].

We obtained the groundwater table (GWL) data from the IndiaWRIS website. IndiaWRIS, which stands for *India Water Resources Information System*, is an Indian government database and information system that tracks and manages water resource data. It contains data on surface water, groundwater, rainfall, and water demand and quality, which makes it a comprehensive tool for water resource management in India.

Our study considered two different periods: the training phase and the testing phase. The training phase covered 70% of the period under study, from 1996 to 2013, i.e., approximately 17.5 years. During this phase, we carefully studied the data and found important patterns and relationships. We used this information to predict ET_o for the testing phase, which covered the remaining 30% of the analyzed horizon, from 2013 to 2020, i.e., about 7.5 years. We then compared the predictions made by our model with the actual ET_o values in order to ascertain its accuracy and reliability. This validation step was crucial in assessing the performance of our model. By adopting this systematic approach (Fig. 2), we aimed to develop a scientifically robust and validated model for predicting ET_o , thus contributing to a deeper understanding of ET_o dynamics within a given time frame.

Methodology

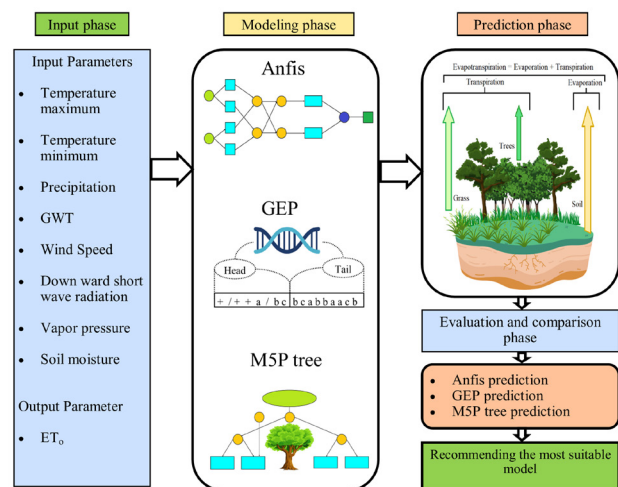


Figure 2. General flowchart of our ET_o modeling, prediction, and evaluation processes
Source: Authors

Descriptions of machine learning models

Adaptive neuro-fuzzy inference system (ANFIS)

The ANFIS model is a powerful tool that allows establishing robust relationships between input and output data. By leveraging fuzzy rules, it effectively learns from a neural network to generate a refined input structure for a given system. This unique model combines the processes of artificial neural networks and fuzzy logic, generating nonlinear maps that precisely define the intricate relationships between input and output spaces. As a neuro-fuzzy system, ANFIS encompasses three fundamental components: fuzzification, an inference engine, and defuzzification. These integrated mechanisms allow optimizing and translating complex data into comprehensible and actionable insights [1].

The proposed inference framework employs a hierarchical structure consisting of five distinct layers, as depicted in Fig. 3. This network architecture encompasses input (layer 0) and yield (layer 5) hubs, which effectively represent the origins of the input and yield variables, respectively. Within the intermediate layers, a combination of predetermined and adaptable hubs serves as the membership functions (MFs) and rules. The ANFIS model incorporates two pivotal knowledge factors, denoted as x and y , while employing a yield variable, represented by z , in order to elucidate the underlying methodology [14]. To establish the relationship between knowledge and yield, the ANFIS model leverages if-then fuzzy rules. Here, input variables representing knowledge factors are fuzzified into linguistic terms and associated with fuzzy sets. Fuzzy rules that reflect the domain's knowledge or data define how these inputs relate to the yield. Fuzzy inference combines input fuzziness, and aggregation weights the rule outputs based on their truth values. Defuzzification converts the aggregated result into a single numerical yield prediction. The key lies in appropriately defining fuzzy rules and membership functions to capture the relationship between inputs (e.g., climate variables) and outputs (e.g., yield or ET_o). In addition, model parameters are tuned during training to fit the data.

Notably, this model encompasses two specific fuzzy rules, which can be expressed in the form proposed by [15]:

$$\text{Rule 1: if } x \text{ is } A_1 \text{ and } y \text{ is } B_1, \text{ then } f_1 = p_1x + q_1y + r_1 \quad (1)$$

$$\text{Rule 2: if } x \text{ is } A_2 \text{ and } y \text{ is } B_2, \text{ then } f_2 = p_2x + q_2y + r_2 \quad (2)$$

As previously mentioned, the ANFIS structure encompasses five distinct layers, each of which plays a crucial role in the fuzzy model. Layer 1, the *fuzzification layer*, transforms crisp input variables into fuzzy linguistic terms, such as A_1 , B_1 , A_2 , and B_2 , capturing the semantic levels of the variables. Layer 2, the *rule layer*, comprises fixed nodes representing specific fuzzy rules. These nodes utilize fuzzy if-then rules to establish relationships between the input and output variables. Moreover, the *normalization layer* (layer 3) features adaptive nodes, denoted by N , which calculate the ratios between rule strengths to combine their effects during

computation. Layer 4, the *defuzzification layer*, determines the final output value, employing nodes that are flexible in converting fuzzy results into precise outputs. Finally, layer 5, the *output layer*, integrates signals from the previous layer to produce the final output of the ANFIS model through a single settled node. Each layer contributes uniquely to the overall functioning and effectiveness of this structure.

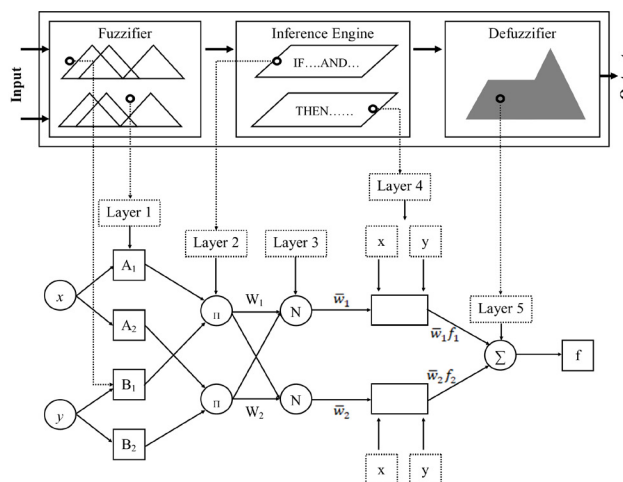


Figure 3. Architecture of the ANFIS model

Source: Authors

In summary, the ANFIS structure employs five layers to convert crisp input variables into fuzzy terms, apply fuzzy rules, normalize rule strengths, defuzzify the results, and calculate the overall yield based on combined signals. The grid partition technique is crucial for constructing Sugeno-type fuzzy inference systems (FISs) using training datasets [15]. The ANFIS creates fuzzy partitions, utilizes rule-based inference, and adapts to data through learning, thereby aiding in segmenting data, recognizing patterns, and handling nonlinear relationships. The grid partition algorithm divides input datasets into distinct fuzzy regions using various MFs, facilitating a comprehensive representation of data patterns. In this regard, MATLAB, a high-level programming language and interactive environment, is an ideal platform for implementing the ANFIS, given its robust capabilities for numerical computing, data analysis, and visualization [16]. Its efficient tools for training and testing ANFIS models, its integration with simulation environments such as Simulink, and its strong user community support make MATLAB a suitable choice for real-world applications [17].

Gene expression programming (GEP)

GEP is an evolutionary computation method that combines the advantages of genetic programming (GP) and genetic algorithms (GAs) while addressing their limitations. It adopts chromosomes as its fundamental data structure and utilizes a concise encoding approach to tackle complex problems. In this technique, a chromosome represents a sequence of genes connected through a linking function. Each gene consists of a head section that contains both functions and terminals and a tail section that only contains terminals. To efficiently handle

complex problems, GEP has a unique feature: the length of the head section (h) is carefully determined for every specific problem, which allows calculating the tail length (t) directly. By organizing and optimizing the genetic information within the chromosomes, GEP can address challenging problems effectively [18].

Fig. 4 shows an example of GEP. In this approach, phenotypic translation involves parsing the functions and terminals in a top-down and left-to-right fashion. This parsing methodology ensures a systematic and sequential interpretation of the genetic information encoded within the chromosome. Moreover, the functions and terminals are arranged hierarchically. This makes it easier to derive the phenotypic expression tree. The top-down and left-to-right approach ensures that the genetic program is translated into a coherent and meaningful mathematical representation, which contributes to a more comprehensive understanding of the encoded relationships and operations. This systematic translation process greatly improves our ability to understand and use GEP models; it makes them more interpretable and useful, allowing researchers to analyze, evaluate, and apply them in different problem domains more effectively. The mathematical expression tree derived from the GEP example is as follows:

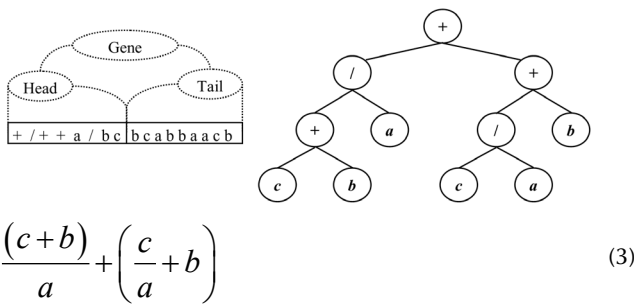


Figure 4. GEP architecture
Source: Authors

GEP utilizes several genetic operators: mutation introduces random changes to gene information, inversion modifies gene heads, transposition rearranges transposable elements, and recombination exchanges gene information between chromosomes. Users set predefined rates for each operator to control their application during evolution.

M5P tree

The M5P tree, developed by Quinlan [19], is a data mining technique employed to establish associations between output (dependent) and input (independent) variables. Also known as the *M5Prime* or *M5' model*, it is a type of decision tree used primarily for regression tasks. It extends the concept of *decision tree*, commonly used for classification and regression, to provide more accurate predictions for continuous numerical target variables. This approach utilizes a binary decision tree structure, where each leaf node incorporates a linear regression function. The structure of the M5P tree model follows a divide-and-conquer approach, resulting in a well-organized and interpretable topology [20], as depicted in Fig. 5.

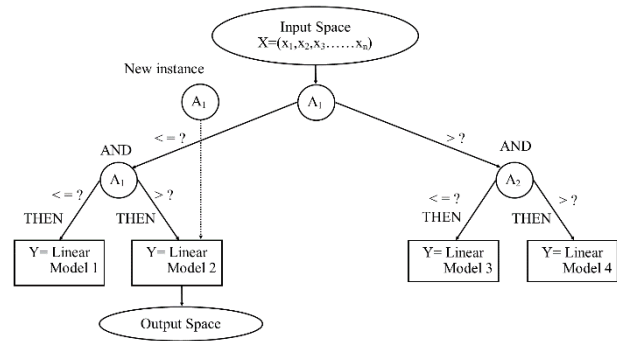


Figure 5. Architecture of the M5P tree
Source: Authors

The process of constructing a decision tree involves two stages. In the first stage, the data are divided into subgroups based on the principle of standard deviation, aiming to minimize the model training error at each node. This splitting process helps to create the decision tree structure [21]. In the second stage, the over-fitted portions of the tree are pruned, eliminating unnecessary complexity. Subsequently, linear regression functions are introduced to replace the pruned subtrees, enhancing the interpretability of the model. Through this methodology, the relationships between variables can be effectively analyzed and modeled, obtaining accurate predictions and valuable insights. The organized structure and pruning techniques of this approach contribute to its robustness, making it an appealing choice for various scientific applications [20]. In summary, M5P employs node splitting and pruning techniques for model construction and simplification, and its prediction accuracy is evaluated using metrics such as R-squared (R²) and the root mean square error (RMSE). Despite its enhanced flexibility, the M5P model is still interpretable thanks to its structure, making it a valuable tool for a wide range of regression tasks.

In recent years, researchers have explored and demonstrated the successful application of the M5P tree to the simulation of various hydrological processes. These include drought forecasting [21], infiltration simulation, river discharge forecasting, reference ETo estimation [20], stage-discharge forecasting, and groundwater level prediction. The versatility of the M5P model in these domains highlights its potential for enhancing our understanding of complex hydrological systems and facilitating informed decision-making [22]. For a comprehensive understanding of the M5P tree and its underlying principles, interested readers are encouraged to consult the works of Quinlan [19], the original developer of this technique.

Assessment criteria and metric formulas for model evaluation

In this study, model effectiveness was assessed using four key metrics: the RMSE, the coefficient of determination (R²), Nash-Sutcliffe efficiency (NSE), and the mean squared error (MSE), each offering unique insights into the performance of our proposal. The RMSE quantifies overall accuracy, with

lower values indicating a better performance. Ranging from 0 to 1, R^2 measures the proportion of variance explained by the independent variables. In addition, NSE assesses variability and bias relative to observed values, with higher values indicating a better performance. Finally, the MSE calculates the average squared differences between observed and predicted values, with lower values indicating greater precision. These metrics collectively provide a thorough evaluation, considering accuracy, explanatory power, and overall performance. Their computation requires two datasets: predicted and observed ET_o values, whose specific equations are outlined below.

$$RMSE = \sqrt{\frac{1}{n} \sum_{i=1}^n (ET_o - ET_p)^2} \tag{4}$$

$$R^2 = \left[\frac{\sum_{i=1}^n (ET_o - \overline{ET_o})(ET_p - \overline{ET_p})}{\sqrt{\sum_{i=1}^n (ET_o - \overline{ET_o})^2} * \sqrt{\sum_{i=1}^n (ET_p - \overline{ET_p})^2}} \right]^2 \tag{5}$$

$$NSE = 1 - \frac{\sum_{i=1}^n (ET_o - ET_p)^2}{\sum_{i=1}^n (ET_o - \overline{ET_o})^2} \tag{6}$$

$$MSE = \frac{\sum_{i=1}^n (ET_o - ET_p)^2}{n} \tag{7}$$

For Korba, Jharsuguda, Bilaspur, Bhubaneswar, and Balangir, the calculations followed a similar approach, using the values from the testing dataset and the provided weights. In this study, we employed a weighted scoring approach to evaluate and determine the optimal alternative among the three models. This is due to the minimal difference observed in the R^2 values and other closely aligned statistical parameters within the models. By assigning appropriate weights to various performance indicators, we could effectively discern the relative strengths and weaknesses of each model, facilitating a more comprehensive assessment of their overall efficacy.

Results

The complete calculations for the scores weighted based on the evaluation metrics of the testing dataset are shown in Tables I and II and presented in Table III.

For Raipur:

- M5P weighted score = (0.4 * 0.9934428) + (0.3 * 0.122735) + (0.15 * 0.995715) + (0.15 * 0.036146) = 0.59095341
- ANFIS weighted score = (0.4 * 0.9998975) + (0.3 * 0.332819) + (0.15 * 0.967497) + (0.15 * 0.000386) = 0.63217211
- GEP weighted score = (0.4 * 0.9859216) + (0.3 * 0.18986) + (0.15 * 0.982737) + (0.15 * 0.00808) = 0.59876071

Table I. R^2 and RMSE of the M5P, ANFIS, and GEP models

Districts	Models	R^2			RMSE		
		Training	Testing	Total dataset	Training	Testing	Total dataset
Raipur	M5P	0.9934428	0.9958844	0.994116	0.091163	0.122735	0.076454
	ANFIS	0.9998975	0.9678599	0.991785	0.003739	0.332819	0.003136
	GEP	0.9859216	0.9829504	0.985005	0.461603	0.18986	0.387124
Korba	M5P	0.994471	0.989528	0.992979	0.196011	0.087204	0.164384
	ANFIS	0.999947	0.974462	0.992658	0.021191	0.22592	0.017772
	GEP	0.987302	0.992212	0.989056	0.03036	0.167802	0.025461
Jharsuguda	M5P	0.996438	0.996556	0.996477	0.143474	0.400698	0.143474
	ANFIS	0.999946	0.990526	0.997363	0.008363	0.31608	0.007014
	GEP	0.969375	0.96661	0.968618	0.239058	0.948186	0.200486
Bilaspur	M5P	0.994123	0.993151	0.993767	0.148018	0.103872	0.124135
	ANFIS	0.999937	0.967727	0.991064	0.020633	0.256653	0.017304
	GEP	0.990346	0.990034	0.990245	0.081506	0.26755	0.068355
Bhubaneswar	M5P	0.991202	0.989462	0.990609	0.008736	0.782929	0.007327
	ANFIS	0.999734	0.930746	0.980326	0.017144	0.116201	0.014378
	GEP	0.971692	0.969294	0.971185	0.052505	0.128649	0.044034
Balangir	M5P	0.995828	0.996817	0.996092	0.149379	0.408665	0.125277
	ANFIS	0.999939	0.961786	0.989525	0.011826	0.101152	0.009918
	GEP	0.987653	0.991485	0.989304	0.087774	0.287071	0.073612

Source: Authors

Table II. NSE and MAE of the M5P, ANFIS, and GEP models

Districts	Models	NSE			MAE		
		Training	Testing	Total dataset	Training	Testing	Total dataset
Raipur	M5P	0.993426	0.995715	0.994112	0.009145	0.036146	0.006432
	ANFIS	0.999898	0.967497	0.991764	0.000146	0.000386	0.000103
	GEP	0.98583	0.982737	0.984882	0.015784	0.00808	0.011102
Korba	M5P	0.994452	0.989417	0.992975	0.012116	0.023429	0.008522
	ANFIS	0.999947	0.972717	0.992527	0.000178	0.002375	0.000125
	GEP	0.987284	0.992129	0.989027	0.014023	0.01987	0.009863
Jharsuguda	M5P	0.9964	0.996219	0.996472	0.000569	0.00793	0.000809355
	ANFIS	0.999946	0.990458	0.997358	5.98E-05	0.004872	4.20787E-05
	GEP	0.969115	0.965943	0.968318	0.10367	0.376165	0.07291426
Bilaspur	M5P	0.994101	0.992973	0.993767	0.016026	0.036638	0.011271477
	ANFIS	0.999937	0.965481	0.990892	0.000339	0.002991	0.000238736
	GEP	0.990342	0.98984	0.990222	0.001503	0.002533	0.001057174
Bhubaneswar	M5P	0.991194	0.989045	0.990591	0.006295	0.016873	0.00442738
	ANFIS	0.999734	0.926792	0.979979	0.000333	0.034319	0.000234046
	GEP	0.971525	0.97113	0.970833	0.005782	0.020787	0.004066537
Balangir	M5P	0.995826	0.996713	0.996078	0.000187	0.024196	0.000131743
	ANFIS	0.999939	0.9593	0.989318	7.77E-05	0.00476	5.46225E-05
	GEP	0.987597	0.991238	0.989248	0.025236	0.06265	0.017749391

Source: Authors

Table III. Weighted score of the M5P, ANFIS, and GEP models

Station	M5P weighted score	ANFIS weighted score	GEP weighted score	Best MODEL
Raipur	0.59095341	0.63217211	0.59876071	ANFIS
Korba	0.59271508	0.64215156	0.61993872	ANFIS
Jharsuguda	0.6380162	0.64011782	0.5436822	ANFIS
Bilaspur	0.59285992	0.63607293	0.61845494	ANFIS
Bhubaneswar	0.59037246	0.57308385	0.59473655	GEP
Balangir	0.64069002	0.60470215	0.61668394	M5P

Source: Authors

The weights of 0.4 for R^2 , 0.3 for the RMSE, 0.15 for NSE, and 0.15 for the MAE were selected to enhance the effectiveness of our model evaluation process. R^2 , assigned the highest weight, is crucial for assessing a model's ability to explain data variance, aligning with our primary research objective. Moreover, RMSE, with its moderate weight, was included to gauge the magnitude of the prediction error, a key consideration for precise forecasting. NSE is valuable for assessing how well a model reproduces the observed variability, which is especially relevant in hydrological and environmental modeling. Finally, the MAE complements the RMSE by providing insights into average prediction errors while being less sensitive to outliers. These weights ensure a well-rounded assessment of model performance, considering both explanatory power and predictive accuracy.

Model performance

ANFIS

The generation of MF combinations for the ANFIS followed a systematic process, which involved selecting different MF types, such as *trim*, *trapmf*, *gbellmf*, *gaussmf*, and *gauss2mf*, based on their appropriateness for the dataset. We experimented with various parameter values within each type to create different MFs, defining their shapes, widths, and centers. The systematic variation of these parameters enabled the exploration of a wide range of MF configurations. These parameterized MFs were then combined into sets representing unique ANFIS model configurations. To thoroughly assess the performance of this

model, a comprehensive evaluation was conducted using several statistical error indices (the RMSE and R^2).

In Table IV, the Raipur district station was employed to test a total of 15 combinations using the available dataset. Each combination represented a unique model configuration. By analyzing the performance of these combinations, we sought to identify the most effective approach for predicting the desired outcome.

Out of the 15 combinations, one using the MF [3, 3, 2, 2, 2, 2, 2, and 2] and *gaussmf* stood out as the most effective. The results obtained from this combination were highly promising. Its R^2 value of 0.991785 was impressive, and its RMSE of 0.003136 was exceptionally low. These outcomes suggest the high predictive accuracy of this specific combination when compared to the other tested alternatives.

Table IV provides a comprehensive overview of the performance of various models used for ETo estimation. Researchers can use this information to select the most suitable ANFIS model configuration for their specific needs while considering its trade-off between accuracy and computational efficiency.

Table IV. Performance of various ANFIS membership functions and membership types

Serial No	Membership function	MF type	Total dataset	
			R^2	RMSE
1	2,2,2,2,2,2,2,2	<i>trim</i>	0.989392	0.017886
2	3,3,2,2,2,2,2,2	<i>trimf</i>	0.991451	0.00485
3	3,3,3,3,2,2,2,2	<i>trimf</i>	0.984223	0.0031
4	2,2,2,2,2,2,2,2	<i>trapmf</i>	0.198024	0.058203
5	3,3,2,2,2,2,2,2	<i>trapmf</i>	0.630894	0.016951
6	3,3,3,3,2,2,2,2	<i>trapmf</i>	0.821287	0.084911
7	2,2,2,2,2,2,2,2	<i>gbellmf</i>	0.988916	0.050455
8	3,3,2,2,2,2,2,2	<i>gbellmf</i>	0.985395	0.029578
9	3,3,3,3,2,2,2,2	<i>gbellmf</i>	0.979612	0.005629
10	2,2,2,2,2,2,2,2	<i>gaussmf</i>	0.986377	0.013078
11	3,3,2,2,2,2,2,2	gaussmf	0.991785	0.003136
12	3,3,3,3,2,2,2,2	<i>gaussmf</i>	0.989151	0.002546
13	2,2,2,2,2,2,2,2	<i>gauss2mf</i>	0.907407	0.080575
14	3,3,2,2,2,2,2,2	<i>gauss2mf</i>	0.902068	0.011761
15	3,3,3,3,2,2,2,2	<i>gauss2mf</i>	0.876112	0.0097

Source: Authors

GEP

Table V shows the results of four attempts to evaluate the performance of the GEP model in predicting ETo data. The number of chromosomes and fitness functions used for modeling varied in each attempt. The goal was to find the most effective combination of parameters for accurately predicting ETo values.

Table V. Performance metrics for the GEP Model

Trial No.	Number of chromosomes	Fitness function	No. of runs	Total dataset	
				R^2	RMSE
1	30	MSE	100 000	0.98725	0.37215
2	50	MSE	100 000	0.97518	0.69685
3	30	RMSE	100 000	0.98906	0.02546
4	50	RMSE	100 000	0.98164	0.05923

Source: Authors

In our GEP model, 30 and 50 chromosomes were employed in conjunction with the fitness functions (RMSE and MSE). The use of 30 chromosomes prioritized computational efficiency, enabling faster convergence and resource conservation. Conversely, the use of 50 chromosomes aimed to explore a broader solution space, enhancing diversity and mitigating premature convergence in complex optimization scenarios. This dual approach strikes a balance between computational efficiency and comprehensive solution exploration, facilitating a thorough evaluation of the algorithm's performance. The fitness functions were chosen because the primary objective was to minimize prediction errors. The MSE assigns greater weight to large errors due to the squaring operation, making it sensitive to outliers, which can be beneficial if the goal is to significantly penalize large errors. On the other hand, the RMSE is advantageous when the goal is to measure the magnitude of the error in the same units as the target variable, since it balances the impact of large and small errors via the square root of the squared errors.

As previously mentioned, the performance of the GEP model was assessed using R^2 and the RMSE. The former indicates how well the model explains the variance in the ETo data, while the latter measures the average difference between the predicted and actual values of the dataset. A lower RMSE indicates a better fit between the predicted and actual ETo values.

Table I shows the R^2 and RMSE values for the complete dataset, which represents the entire range of ETo data used in this study. Furthermore, the parameters of the optimized GEP model are shown in Table V. These values can be used to assess the accuracy and reliability of GEP in predicting ETo across different runs. A careful examination of our results revealed that trial 3 was the most favorable choice; it had lower error rates in terms of both R^2 and RMSE than the other trials. This means that it achieved greater accuracy and precision in modeling ETo. In light of the above, a head size of 8 was deemed optimal.

In summary, Table V shows that trial number 3 was the most effective approach for predicting ETo. This trial had the highest R^2 value (0.98906) and the lowest RMSE (0.02546), which indicates that it was able to capture the variability of the ETo data and minimize prediction errors.

M5P tree

The prediction models constructed using the M5P algorithm were implemented using the WEKA tool. To create these models, the dataset was divided into two subsets: 70% for training and 30% for testing. The M5P tree uses linear regression to generate mathematical expressions that capture the different data classes. This allows the model to make predictions about new data similar to those on which it was trained.

The different linear regression models (LMs) were generated from the M5P model for the ETo data. This technique offers flexibility with its piecewise linear regression, adapting to complex data patterns, while traditional linear regression assumes a single global linear relationship, which may not effectively capture nonlinearity. M5P enhances adaptability, making it suitable for intricate datasets, while traditional linear regression prioritizes simplicity and interpretability. The equations in the table represent the linear regression relationships established by the M5P tree. Furthermore, Fig. 6 illustrates the structure and hierarchy of the model based on the equations derived from the M5P algorithm.

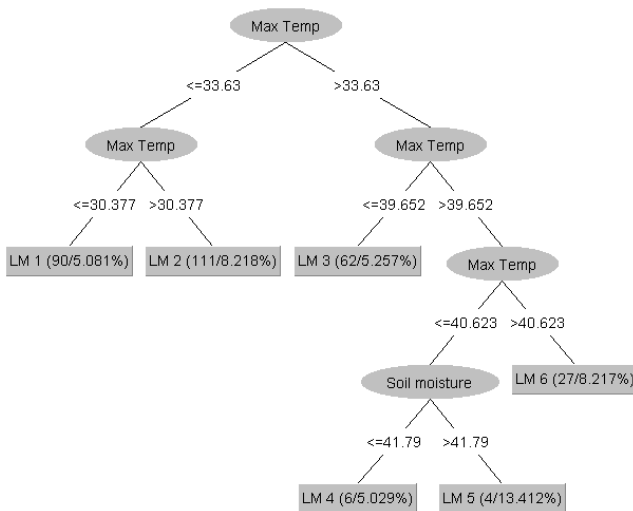


Figure 6. Regression tree generated via ten-fold cross-validation of the M5P tree

Source: Authors

Comparing the models

We conducted a comprehensive analysis of the M5P, ANFIS, and GEP models in predicting actual ETo values using the provided dataset. As previously mentioned, we considered multiple evaluation metrics (R^2 , RMSE, NSE, and MAE) for the testing dataset. According to the results, ANFIS consistently outperformed the other models across multiple stations. It achieved high values of R^2 (ranging from 0.930746 to 0.990526) and NSE (from 0.926792 to 0.990458), indicating strong correlation and agreement between the predicted and observed ETo values. Additionally, ANFIS had the lowest RMSE (0.101152-0.332819) and MAE (0.000386-0.034319) among the tested models. These low error values indicate the model's accuracy and precision in estimating ETo,

and its consistent performance and superior metrics bear witness to its reliability.

Table III shows the weighted scores of different models for predicting actual ETo at various stations, with higher values reflecting better predictive capability. In all stations, ANFIS consistently exhibited a strong performance, achieving the highest weighted score in most locations (e.g., Raipur, Korba, Jharsuguda, and Bilaspur). These results suggest that ANFIS is a reliable and effective model for ETo prediction in these regions.

However, there are some exceptions in the table. For the Bhubaneswar station, GEP achieved the highest weighted score, which indicates its superior performance compared to M5P and ANFIS. This implies that GEP may be a more suitable choice for ETo prediction in the specific context of Bhubaneswar.

The Balangir station represents a unique scenario since M5P obtained the highest weighted score among the three models, suggesting that it may be a better model for predicting ETo in the region. More research is needed to confirm this, but M5P is a promising, versatile, and adaptable model for predicting ETo that could outperform ANFIS and GEP in some regions of the Mahanadi Basin.

ANFIS is the clear winner regarding ETo prediction: it consistently performs better than the other two models across multiple stations. This makes it a valuable tool in a variety of different settings. However, the best choice for predicting ETo may vary from station to station. For example, GEP performed exceptionally well in Bhubaneswar, while M5P performed well in Balangir. These findings highlight the importance of selecting models that are tailored to the unique characteristics of each location.

Scatterplots were used to determine how closely the predicted ETo values matched the observed data (Figs. 7, 8, and 9). The closer the points on the scatterplot are to a straight line, the better the model is at predicting ETo. The three models were compared through these scatterplots with the help of the statistical parameters. The results for ANFIS at Raipur, Korba, Jharsuguda, and Bilaspur show a strong correlation between the observed and predicted ETo values. The points on the scatterplots are tightly clustered around the diagonal line, which indicates that the model is doing a good job of predicting ETo, effectively capturing variations and providing accurate predictions. In contrast, the scatterplots for Bhubaneswar and Balangir display a relatively tighter alignment between the observed ETo values and the predictions of the GEP and M5P models. The points on these scatterplots show proximity to the diagonal line, indicating good agreement between the predicted and observed ETo values. This suggests that the GEP and M5P models perform well in estimating ETo at these two stations. However, it is worth noting that the scatterplots for all the stations show some scattered points that deviate from the diagonal line, evidencing some level of prediction error.

These scatterplots clearly illustrate the alignment between observed and predicted ETo values for all three models across six stations.

The ANFIS plots show points tightly clustered along the diagonal line, indicating a high prediction accuracy. In contrast, GEP and M5P show a better fit only at specific

stations. These figures support the conclusion that ANFIS performs consistently across locations, while GEP and M5P show location-specific effectiveness, reinforcing the model selection rationale discussed in this work. The observed outliers might be influenced by various factors such as measurement errors, environmental variability, or model limitations.

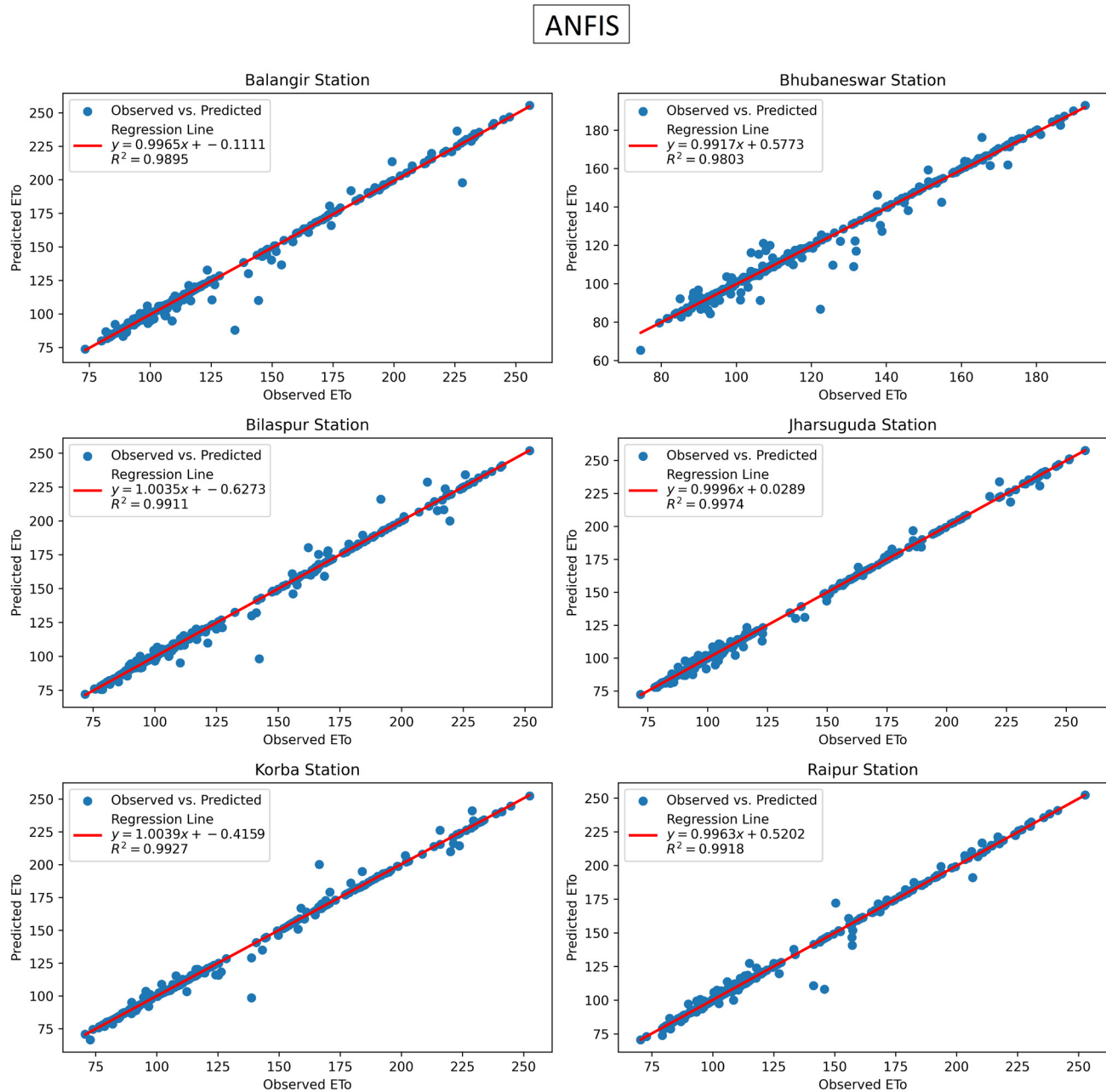


Figure 7. Scatterplots depicting the relationship between the observed and predicted ETo values obtained by using the ANFIS on the Raipur, Korba, Jharsuguda, Bilaspur, Bhubaneswar, and Balangir stations

Source: Authors

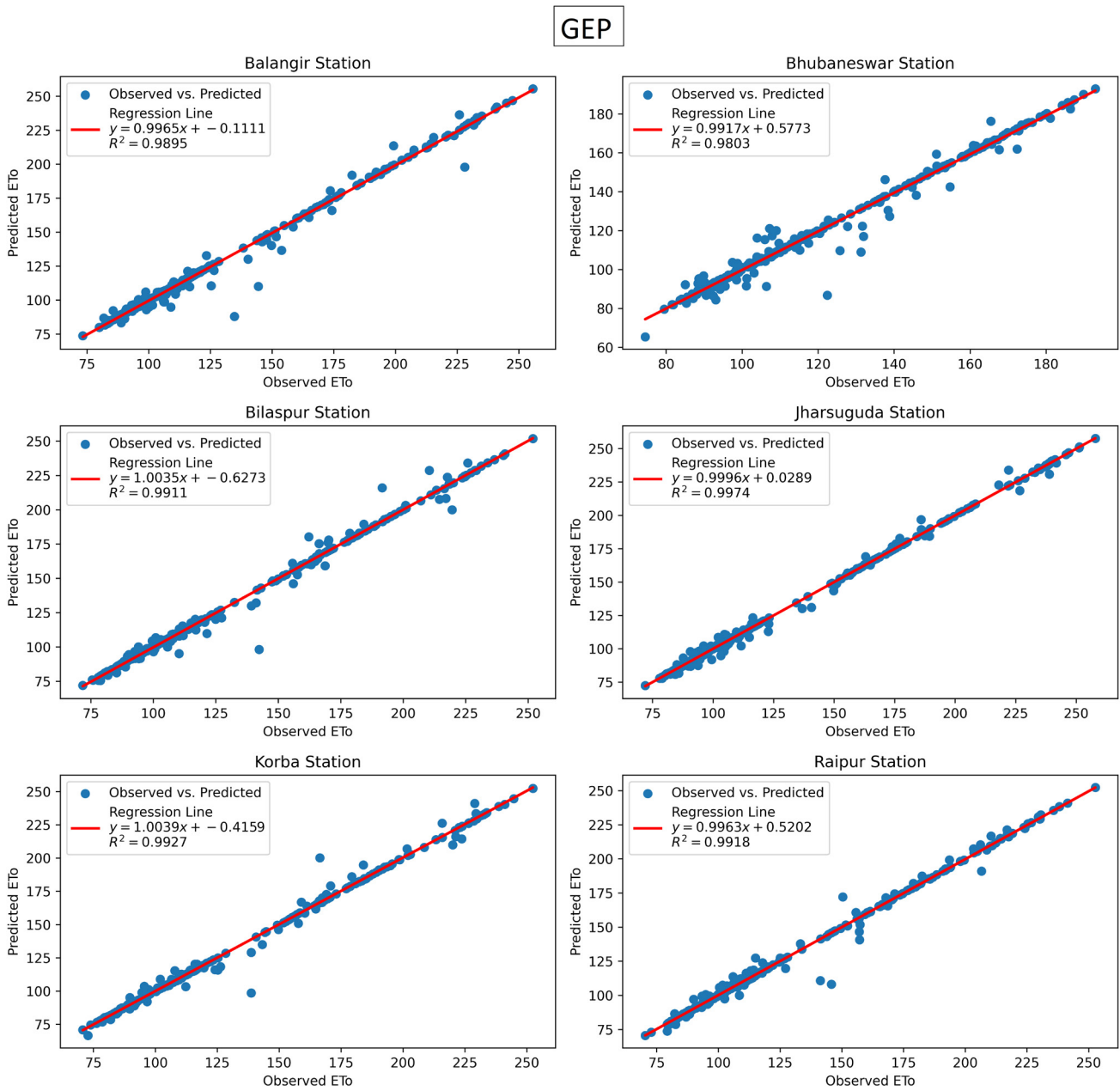


Figure 8. Scatterplots depicting the relationship between the observed and predicted ETo values obtained by using the GEP model on the Raipur, Korba, Jharsuguda, Bilaspur, Bhubaneswar, and Balangir stations
Source: Authors

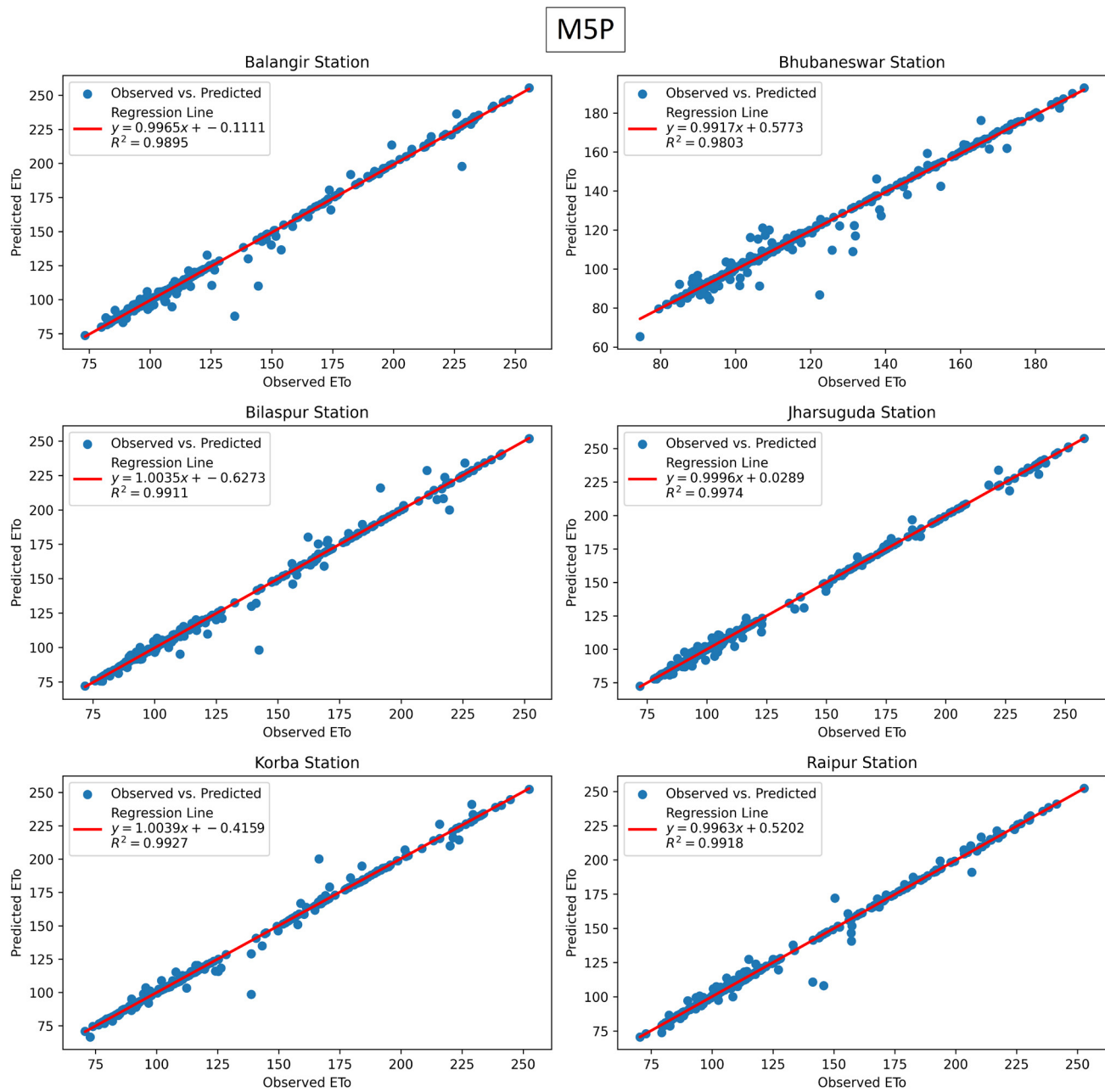


Figure 9. Scatterplots depicting the relationship between the observed and predicted ETo values obtained by using the M5P model on the Raipur, Korba, Jharsuguda, Bilaspur, Bhubaneswar, and Balangir stations
Source: Authors

Discussion

Within the field of ETo modeling, various studies have explored the efficacy of both simple and hybridized AI approaches, as outlined in the introductory section. Notable among these studies are the works of [1], [7], [8], [10], and [23]. These works have demonstrated the effectiveness of combining AI techniques for the accurate prediction of ETo, which aligns with our findings. By merging different AI methodologies such as machine learning algorithms and neural networks, these studies have exemplified the potential of AI-driven approaches in improving ETo modeling and enhancing our understanding of its intricate dynamics.

Our use of the ANFIS yielded remarkable results, as also reported by [24], in the form of high R^2 (0.930746-0.990526) and NSE (0.926792-0.990458) values. These values signify robust correlation and agreement between the predicted and observed ETo values. Notably, ANFIS outperformed the other models; it obtained the lowest RMSE (0.101152-0.332819) and MAE (0.000386-0,034319). These findings highlight the exceptional accuracy and predictive capability of the ANFIS model when it comes to ETo modeling, estimation, and forecasting.

The superior performance of the ANFIS model may be attributed to its hybrid architecture, which combines the learning capability of neural networks with the reasoning of fuzzy logic, allowing it to effectively capture the complex nonlinear relationships inherent in ETo data. In contrast, M5P's success in Balangir could be due to its strength in modeling piecewise linear relationships, which may align better with the local data characteristics. On the other hand, GEP, with its evolutionary approach, offers robustness and generalizability. This may explain its relative success in Bhubaneswar, where environmental conditions may exhibit higher variability.

The analysis of the dataset and the evaluation of different models for predicting ETo provided significant insights into their performance. The weighted scores obtained helped to comprehensively assess the models' predictive capabilities. M5P exhibited remarkable performance in estimating ETo, as also reported by [4] while also using its hybridized versions (AR-RSS, AR-M5P, RSSM5P, and AR-RSS-M5P). The GEP model performed slightly worse than ANFIS and M5P in terms of the NSE and MAE. Nevertheless, its overall performance suggests that it can be a valuable tool for ETo prediction, particularly in locations where ANFIS may not be the optimal choice.

Additionally, the scatterplots presented herein illustrate the alignment between the observed ETo values and the predictions of the ANFIS and M5P models, indicating their ability to capture variations. However, some scattered outliers suggest the presence of prediction errors, which could be influenced by measurement inaccuracies or other environmental factors. Overall, this study underscores

the importance of choosing appropriate models for ETo prediction, with ANFIS emerging as the preferred alternative because of its consistent and accurate estimations.

Practical implications

This study provides actionable insights for model selection in ETo prediction. The ANFIS, while computationally intensive due to its training structure, is highly suitable for regions with complex nonlinear climatic interactions and sufficient training data. Conversely, the M5P model, with its simpler and interpretable structure, is ideal for data-scarce environments or operational settings requiring faster computation. The GEP model shows robustness in highly variable climate zones such as Bhubaneswar, making it suitable where generalizability is essential. These distinctions offer valuable guidance to researchers and policymakers in selecting the appropriate model based on data availability, climatic variability, and computational capacity.

Conclusions

This study explored the prediction of actual ETo values by means of multiple models, evaluating their performance based on rigorous statistical analysis. The findings underscore the significance of selecting an appropriate model for accurate ETo estimation, which is crucial for effective water resource management and agricultural planning. ANFIS was the clear winner among the evaluated models, consistently outperforming M5P and GEP. This suggests that ANFIS is better at capturing the complex relationships between the input variables and ETo. M5P and GEP also performed well, but ANFIS had higher R^2 , lower RMSE, higher NSE, and lower MAE values, indicating that it is more robust and accurate at predicting ETo in the Mahanadi Basin. The scatterplots showed that the ANFIS model is able to predict ETo values quite accurately, with most of the points clustering closely around the diagonal line. However, there were a few outliers, which suggests that there may be a few sources of error in the data or the model. These errors could be caused by measurement inaccuracies, environmental complexities, or other factors, but they can be neglected. This study revealed that machine learning can be used to improve the accuracy of ETo predictions. With more accurate predictions, researchers, water managers, and farmers can make better decisions regarding water allocation and crop management.

Future research could focus on refining the models and adding more factors to improve their predictive performance as well as the accuracy of ETo estimates. The findings of this study highlight the effectiveness of the ANFIS as a valuable tool in different locations. This could be helpful for water resource management, irrigation planning, and agricultural decision-making. Other works could focus on optimizing and fine-tuning the parameters of the ANFIS model, enhancing its performance and making it applicable in a broader range of contexts.

Acknowledgements

The data for this study were obtained from TerraClimate (<https://www.climateengine.org/>), and the GWT data were gleaned from the IndiaWRIS portal (<https://indiawris.gov.in/wris/#/>).

CRedit author statement

Gopikrishnan T. conceived the idea and conducted the background research. *Deepak Kumar Raj* collected the data, developed the workflow, and performed the assessment. *Gopikrishnan T.* supervised the research and provided critical feedback. *Deepak Kumar Raj* led the manuscript's writing process and wrote its main part, to which the other authors contributed.

Conflicts of interest

The authors declare no conflicts of interest.

References

- [1] P. Aghelpour, V. Varshavian, M. Khodamorad Pour, and Z. Hamed, "Comparing three types of data-driven models for monthly evapotranspiration prediction under heterogeneous climatic conditions," *Sci. Rep.*, vol. 12, no. 1, art. 22272 Dec. 2022. <https://doi.org/10.1038/s41598-022-22272-3>
- [2] D. K. Roy, R. Barzegar, J. Quilty, and J. Adamowski, "Using ensembles of adaptive neuro-fuzzy inference system and optimization algorithms to predict reference evapotranspiration in subtropical climatic zones," *J. Hydrol.*, vol. 591, art. 125509, Dec. 2020. <https://doi.org/10.1016/j.jhydrol.2020.125509>
- [3] H. Dehghanisani, H. Emami, S. Emami, and V. Rezaverdinejad, "A hybrid machine learning approach for estimating the water-use efficiency and yield in agriculture," *Sci. Rep.*, vol. 12, no. 1, art. 10844, Dec. 2022. <https://doi.org/10.1038/s41598-022-10844-2>
- [4] A. Elbeltagi et al., "Estimating the standardized precipitation evapotranspiration index using data-driven techniques: A regional study of Bangladesh," *Water*, vol. 14, no. 11, art. 1764, Jun. 2022. <https://doi.org/10.3390/w14111764>
- [5] A. S. Azad et al., "Water level prediction through hybrid SARIMA and ANN models based on time series analysis: Red Hills Reservoir case study," *Sustainability*, vol. 14, no. 3, art. 1843, Feb. 2022. <https://doi.org/10.3390/su14031843>
- [6] A. Ashrafzadeh, O. Kisi, P. Aghelpour, S. M. Biazar, and M. A. Masouleh, "Comparative study of time series models, support vector machines, and gmdh in forecasting long-term evapotranspiration rates in northern Iran," *J. Irrig. Drain. Eng.*, vol. 146, no. 6, Jun. 2020, art. 04020005. [https://doi.org/10.1061/\(asce\)ir.1943-4774.0001471](https://doi.org/10.1061/(asce)ir.1943-4774.0001471)
- [7] J. Wang et al., "Development of monthly reference evapotranspiration machine learning models and mapping of Pakistan—A comparative study," *Water*, vol. 14, no. 10, art. 1666, May 2022. <https://doi.org/10.3390/w14101666>
- [8] S. Mehdizadeh, B. Mohammadi, Q. B. Pham, and Z. Duan, "Development of boosted machine learning models for estimating daily reference evapotranspiration and comparison with empirical approaches," *Water*, vol. 13, no. 24, art. 3489, Dec. 2021. <https://doi.org/10.3390/w13243489>
- [9] M. Poursaeid, A. H. Poursaeid, and S. Shabanlou, "A comparative study of artificial intelligence models and a statistical method for groundwater level prediction," *Water Resour. Manage.*, vol. 36, no. 5, pp. 1499–1519, Mar. 2022. <https://doi.org/10.1007/s11269-022-03070-y>
- [10] R. M. Adnan, R. Mostafa, A. R. M. T. Islam, O. Kisi, A. Kuriqi, and S. Heddam, "Estimating reference evapotranspiration using hybrid adaptive fuzzy inferencing coupled with heuristic algorithms," *Comput. Electron. Agric.*, vol. 191, Dec. 2021, art. 106541. <https://doi.org/10.1016/j.compag.2021.106541>
- [11] R. K. Jaiswal, A. K. Lohani, and R. V. Galkate, "Rainfall and agro related climate extremes for water requirement in paddy grown Mahanadi Basin of India," *Agric. Res.*, vol. 12, no. 1, pp. 20–31, Mar. 2023. <https://doi.org/10.1007/s40003-022-00629-4>
- [12] S. Samantaray, A. Sahoo, and A. Agnihotri, "Assessment of flood frequency using statistical and hybrid neural network method: Mahanadi River Basin, India," *J. Geol. Soc. India*, vol. 97, no. 8, pp. 867–880, Aug. 2021. <https://doi.org/10.1007/s12594-021-1785-0>
- [13] J. T. Abatzoglou, S. Z. Dobrowski, S. A. Parks, and K. C. Hegewisch, "TerraClimate, a high-resolution global dataset of monthly climate and climatic water balance from 1958–2015," *Sci. Data*, vol. 5, art. 170191, Jan. 2018. <https://doi.org/10.1038/sdata.2017.191>
- [14] A. Choudhary, B. S. Das, K. Devi, and J. R. Khuntia, "ANFIS and GEP-based model for prediction of scour depth around bridge pier in clear-water scouring and live-bed scouring conditions," *J. Hydroinform.*, vol. 25, no. 3, pp. 1004–1028, May 2023. <https://doi.org/10.2166/hydro.2023.212>
- [15] T. Takagi and M. Sugeno, "Fuzzy identification of systems and its applications to modeling and control," *IEEE Tran. Syst. Man Cyber.*, vol. SMC-15, no. 1, pp. 116–132, Jan.–Feb. 1985. <https://doi.org/10.1109/TSMC.1985.6313399>
- [16] C. Warren, "MATLAB for engineers: Development of an online, interactive, self-study course," *Eng. Educ.*, vol. 9, no. 1, pp. 86–93, 2014. <https://doi.org/10.1112/ened.2014.00026>
- [17] M. Lasheen and M. Abdel-Salam, "Maximum power point tracking using Hill Climbing and ANFIS techniques for PV applications: A review and a novel hybrid approach," *Energy Convers. Manage.*, vol. 171, no. March, pp. 1002–1019, 2018. <https://doi.org/10.1016/j.enconman.2018.06.003>
- [18] R. Zhang and X. Xue, "A new model for prediction of soil thermal conductivity," *Int. Commun. Heat Mass Transf.*, vol. 129, art. 105661, Dec. 2021. <https://doi.org/10.1016/j.icheatmasstransfer.2021.105661>
- [19] A. Adams and L. Sterling, Eds. AI '92. Singapore: World Scientific, 1992. doi: 10.1142/1897

- [20] M. Pal and S. Deswal, "M5 model tree based modeling of reference evapotranspiration," *Hydrol. Process.*, vol. 23, no. 10, pp. 1437–1443, May 2009. <https://doi.org/10.1002/hyp.7266>
- [21] M. Ali, R. C. Deo, N. J. Downs, and T. Maraseni, "An ensemble-ANFIS based uncertainty assessment model for forecasting multi-scalar standardized precipitation index," *Atmos. Res.*, vol. 207, art. 5771, November 2017, pp. 155–180, 2018. <https://doi.org/10.1016/j.atmosres.2018.02.024>
- [22] P. Rai, P. Kumar, N. Al-Ansari, and A. Malik, "Evaluation of machine learning versus empirical models for monthly reference evapotranspiration estimation in Uttar Pradesh and Uttarakhand States, India," *Sustainability*, vol. 14, no. 10, art. 5771, May 2022. <https://doi.org/10.3390/su14105771>
- [23] M. Kadkhodazadeh, M. V. Anaraki, A. Morshed-Bozorgdel, and S. Farzin, "A new methodology for reference evapotranspiration prediction and uncertainty analysis under climate change conditions based on machine learning, multi criteria decision making and Monte Carlo methods," *Sustainability*, vol. 14, no. 5, art. 2601, Mar. 2022. <https://doi.org/10.3390/su14052601>
- [24] D. K. Roy, A. Lal, K. K. Sarker, K. K. Saha, and B. Datta, "Optimization algorithms as training approaches for prediction of reference evapotranspiration using adaptive neuro fuzzy inference system," *Agric. Water Manag.*, vol. 255, art. 107003, Sep. 2021. <https://doi.org/10.1016/j.agwat.2021.107003>